

Supporting Information

RNA Hairpin Folding in the Crowded Cell

*Mimi Gao⁺, David Gnutz⁺, Axel Orban, Bettina Appel, Francesco Righetti, Roland Winter, Franz Narberhaus, Sabine Müller, and Simon Ebbinghaus**

anie_201510847_sm_miscellaneous_information.pdf

Supporting Information

Materials and Methods

Synthesis and labeling of 4U and Im-4U RNA. RNA was chemically synthesized on a GeneAssembler (Pharmacia) using phenoxyacetyl (PAC) protected β -cyanoethyl-(*N,N*-diisopropyl)-phosphoramidites of 5'-*O*-dimethoxytrityl-2'-*O*-tertbutyldimethylsilyl (TBDMS) nucleosides as described previously.¹ Both, 4U RNA and its G12A-C23U variant (Im-4U RNA) were modified at the 5'-terminus with an amino linker using C6-NH₂ phosphoramidite, and at the 3'-terminus with an alkinyl group using 2'-*O*-propargyluridine-3'-Icaa on CPG 1000 Å as support. RNA was purified on a 15% denaturing polyacrylamide gel, product containing bands were cut from the gel, and RNA was eluted (0.3 M NaOAc, pH 7.1) followed by ethanol precipitation. Dye labeling was performed with Atto488 NHS-ester and Atto565-azide (ATTO-TEC) in a one-pot reaction. Atto488 NHS-ester (300 μ g) was solved in 60 μ L dry DMF and added to RNA (12 nmol) in 100 μ L sodium carbonate buffer (0.2 M, pH 8.5). Reaction was allowed to proceed for 4 h at 25 °C. Subsequently, Atto488-labeled RNA was added to 100 μ g dry Atto565-azide. A mixture of 100 μ L CuSO₄ (1 mM in phosphate buffer 0.1 M, pH 7) and 100 μ L tris(3-hydroxypropyl)triazolylmethylamine (5 mM in phosphate buffer 0.1 M, pH 7) was saturated with argon for 5 min and added to the RNA solution which was again degassed with argon for 5 min. 125 μ L of freshly prepared sodium ascorbate solution (8 mM) was saturated with argon for 10 min and added to the reaction mixture. Finally, 480 μ L phosphate buffer (0.1 M, pH 7) were added to the solution. After incubation for 4 h at 37 °C RNA was precipitated from ethanol and the double labeled product was isolated by RP-HPLC (EC 250/4 Nucleodur 100-5 C18, *cv* = 3.142 mL) with buffer A (0.1 M TEAAc, 5% acetonitrile) and buffer B (0.1 M TEAAc, 30% acetonitrile) with a four step gradient at a flow rate of 0.5 mL/min: 0% buffer B for 2 *cv*, 50% buffer B for 5 *cv*, 80% buffer B for 25 *cv* and 100% buffer B for 2 *cv*. Double labeled RNA eluated at 68% buffer B. The isolated sample was desalted by gel filtration to give an average amount of 3 nmol of double labeled RNA (Fig. S1).

Preparation of crowding solutions. The crowding reagents sucrose, Ficoll® PM 70, EG, PEG 200, PEG 400, PEG 6k, and PEG 20k were purchased from Sigma-Aldrich. Differently concentrated crowding solutions were prepared in Dulbecco's phosphate-buffered saline (DPBS, pH 7.4).

Vapor pressure osmometry. Changes of water activity were determined by vapor osmometry as described previously.² Briefly, 10 μ L of the crowder solution were applied for measurements to a Wescor 5520 vapor pressure osmometer. The water activity, a_w , relates to the measured osmolality (mOsm [10^{-3} mol/kg]) by $mOsm = -(10^6 \ln a_w)/M_1$, with M_1 being the molecular mass [g/mol] of water.

Cell culture. HeLa cells were grown in 35-mm glass-bottom dishes (FluoroDish, WPI) in DMEM supplemented with 10% FBS, 100U/mL penicillin, and 0.1 mg/mL streptomycin. Prior to microinjection and imaging, the medium was removed and replaced by Leibovitz's L15 medium supplemented with 30% FBS.

Microinjection. Semi-automatic microinjections were performed using an Eppendorf FemtoJet attached to Eppendorf InjectMan NI2 micromanipulator. 3 μ L of 200 μ M FRET-

labeled 4U RNA dissolved in ddH₂O were loaded to a Femtotips II glass-capillary (Eppendorf) from the back using microloader capillaries (Eppendorf). Injection pressure was adjusted to 100-250 hPa for 0.2-0.7 s so that no visible expansion of cell volume was observed during injection.

Sample preparation for FReI. Stock solution of FRET-labeled 4U RNA sample was heated up to 70°C for 5 min and slowly cooled down to RT to ensure correct folding of the RNA hairpin structure. For *in vitro* measurements, 5 μM samples were prepared by mixing the RNA with different crowding solutions. 20 μL of each mixture were placed between a glass bottom dish (FluoroDish, WPI) and a glass cover slip using a 100 μm imaging spacer (Sigma-Aldrich). The dish was then placed on the microscope stage and the excitation light was focused onto the imaging spacer which represents the solution layer. Comparative in-cell measurements were performed in the same way. After removing the medium a glass cover slip with 80 μL Leibovitz's L15 medium supplemented with 30% FBS was mounted via an imaging spacer onto the glass bottom dish which contained microinjected cells. The RNA stock solution was used directly as microinjection sample.

FReI measurement. The principles of Fast Relaxation Imaging (FReI) were described earlier.³⁻⁵ In this study, an inverted fluorescence microscope (AxioObserver Z1, Zeiss) with a Colibri excitations system was used. The monochromatic light was guided through a 90° reflection using a beamsplitter (DFT 490+575, Zeiss) to a 40x objective (N.A. = 0.95, Zeiss) and focused on the sample. Emitted fluorescence of Atto488 and Atto565 was transmitted through the first beamsplitter and was reflected by a prism to the second beamsplitter (BC 565, Zeiss), where donor and acceptor/FRET fluorescence light were separated and reflected onto different CCD cameras (AxioCam HS, Zeiss) with appropriate emission filters (BP512/30 and BP630/98, Zeiss). As described previously,⁵ a diode laser (m2k laser; λ = 2200 nm) was used to induce fast 2.4 °C-temperature jumps, heating the cells and the entire field of view (40x objective; N.A. = 0.95) homogenously. For each jump the temperature was equilibrated for 20 s. The temperature jumps were calibrated using the temperature-sensitive dye rhodamine B.⁵ During temperature jump stepping, the power profile of the diode laser was controlled by a custom-written LabView template. The LED excitation intensity was kept constant for all experiments. Images were recorded with 2 fps using the imaging software AxioVision 4.8 (Zeiss).

Data evaluation. The recorded images were exported as TIFF files for data evaluation in ImageJ (US National Institutes of Health). The fluorescence intensity of donor (D) and acceptor (A) channel were readout for each pixel and averaged over the region of interest (ROI). Afterwards, the D/A ratio was calculated by dividing the donor by the acceptor intensity. The equilibrated D/A-value of each temperature jump (average of 2 frames at 18 s) is plotted against the temperature. We assume a two-state transition for RNA unfolding between folded, *F*, and unfolded, *U*, states. The fraction of the folded state is defined by:

$$f_f = \frac{K}{1+K} \quad (1)$$

where *K* is the equilibrium constant for the unfolding reaction which is defined by:

$$K_u = \frac{[U]}{[F]} \quad (2)$$

where [F] and [U] are the concentrations of the folded and unfolded states, respectively. To account for the intrinsic temperature dependence of both dyes Atto488 and Atto565 (Fig. S2) two linear baselines with the same slope representing the folded ($a_f+b(T-T_{min})$) and unfolded ($a_u+b(T-T_{min})$) state were used, respectively:

$$\frac{D}{A}(T) = \frac{[a_f+b(T-T_{min})]+[a_u+b(T-T_{min})]\cdot K}{1+K} \quad (3)$$

The standard free energy of unfolding is defined by:

$$\Delta G^\circ_u = -RT \ln K_u \quad (4)$$

Considering the temperature dependence of ΔG°_u , the Gibbs-Helmholtz equation was used:

$$\Delta G^\circ_u(T) = \Delta H^\circ_u \left(1 - \frac{T}{T_m}\right) - \Delta C^\circ_p \left[(T_m - T) + T \ln\left(\frac{T}{T_m}\right)\right] \quad (5)$$

where T_m is the melting temperature, ΔH° the standard enthalpy change and ΔC°_p the standard heat capacity change upon unfolding. The difference in heat capacity between the folded and unfolded states was neglected and Eq. (5) was simplified as:

$$\Delta G^\circ_u \approx -\frac{\Delta H^\circ_u}{T_m} \cdot (T - T_m) \quad (6)$$

The standard free energy for unfolding, ΔG°_u , at $T = 310$ K (37 °C) was obtained by

$$\Delta G^\circ_u(310 \text{ K}) = -\frac{\Delta H^\circ_u}{T_m} \cdot (310 \text{ K} - T_m) \quad (7)$$

Fitting and student t-tests were carried out using Origin9 (OriginLab Corporation) and GraphPad Prism 6 (GraphPad Software), respectively.

If considering the equilibrium for RNA folding from a single strand accompanied by water uptake only, the number of water molecules released upon RNA unfolding Δn_w was obtained using Eq. 8:⁶

$$\Delta n_w = \frac{\partial \Delta G^\circ_u(310 \text{ K})}{RT \partial \ln a_w} \quad (8)$$

where R is the gas constant and T is the absolute temperature. Δn_w and the error value were calculated from the slope of a linear fit weighted by the errors in ΔG°_u . An analysis of covariance (ancova) reveals that the differences between the slopes obtained for sucrose and Ficoll 70 are not significant and thus an global slope was calculated with a correction coefficient $r^2 > 0.99$. The dotted line for PEG in Figure 2A shows a correction coefficient $r^2 > 0.93$. The numbers of water molecules released upon lm-4U RNA unfolding, Δn_w , are 91 ± 3 for sucrose/Ficoll and 33 ± 5 for PEG < 6 kDa.

To verify the significant deviation for PEG 6 kDa and 20 kDa from the linear regression shown in Figure 2A, one sample t-tests with a 95% confidence interval against the interpolated free energy values at the experimentally determined water activities were performed. The p-values for PEG 6kDa and 20 kDa are $p = 0.0063$ and $p = 0.0054$, respectively. We further considered the error of a linear interpolation and tested the experimental values against the upper bound of the error. The difference was shown to be significant for PEG 6k ($p=0.0113$) and PEG 20k ($p=0.0075$) showing that PEG 6k and 20k differ significantly from the linear behavior of $\ln a_w$ versus ΔG_u° .

For single pixel evaluation, donor and acceptor images (TIFF) were background subtracted and aligned using ImageJ (NIH). For every time point, a D/A ratio map was generated by dividing donor images by the acceptor images. The TIFF files were then imported into Matlab and thermodynamic analysis was performed for every pixel. For every temperature step, 10 frames were averaged and the mean was used for thermodynamic fitting using Eq. (3). Only fits with errors of T_m below 1 °C were used for the generation of the map. Typical fit errors in cells were in the range of 0.5 ± 0.2 °C and therefore well below the observed variation. We further estimated the intrinsic error of the analysis by a comparative 30×30 px² region in vitro. From the single pixel analysis we obtained a melting temperature of 46.5 ± 0.1 °C and an unfolding free energy (at 37°C) of 5.3 ± 0.2 kJ/mol. We estimated the width of the variation by two standard deviations accounting for 95% of the variation. Thus, the intrinsic noise of the analysis falls within the range of ~ 0.2 k_BT. The intracellular variations are therefore an order of magnitude above the experimental error. Histograms visualizing all single pixel measurements were extracted using ImageJ and then plotted using Graphpad Prism 6.

Gel electrophoresis and EtBr staining. The FRET temperature jump stepping was simulated in a PCR machine with a heat rate of 4 °C/s (T100 Thermal Cycler, Biorad). The RNA was purified by three consecutive extractions with phenol, phenol-chloroform, chloroform, respectively, and ethanol precipitation. 150 ng of the 4U RNA was separated on 10% polyacrylamide gels containing 7 M urea. RNAs were visualized by staining the gels with ethidium bromide.

Supplementary Tables and Figures

Table S1. Melting temperature, T_m , and free energy, ΔG_u° , for unfolding at 37°C of the 4U RNA hairpin in DPBS buffer containing different crowding agents. If not otherwise specified, $n = 4$. Errors indicate mean \pm s.d.

| | $T_m / ^\circ\text{C}$ | $\Delta G_u^\circ (37^\circ\text{C}) / \text{kJ mol}^{-1}$ |
|---------------------------|------------------------|--|
| wildtype (4U) | | |
| low ionic buffer* | 46.2 ± 1.2 | 7.0 ± 0.4 |
| DPBS, pH 7.4 | 52.7 ± 1.6 | 9.9 ± 0.5 |
| G12A-C23U (lm-4U) | | |
| low ionic buffer* | 37.9 ± 0.4 | 0.5 ± 0.2 |
| DPBS, pH 7.4 | 47.4 ± 0.6 | 5.9 ± 0.8 |
| + 100 g/L sucrose | 44.8 ± 0.8 | 4.8 ± 0.3 |
| + 200 g/L sucrose | 42.0 ± 1.0 | 3.0 ± 0.6 |
| + 300 g/L sucrose | 39.7 ± 1.3 | 1.4 ± 0.6 |
| + 100 g/L Ficoll 70 | 47.1 ± 1.2 | 6.1 ± 0.6 |
| + 200 g/L Ficoll 70 | 46.7 ± 1.7 | 5.9 ± 0.9 |
| + 300 g/L Ficoll 70 | 46.2 ± 0.7 | 5.6 ± 0.4 |
| + 300 g/L EG | 35.2 ± 0.7 | -1.2 ± 0.6 |
| + 300 g/L PEG 200 | 37.9 ± 0.7 | 0.5 ± 0.4 |
| + 300 g/L PEG 400 | 42.9 ± 0.5 | 3.7 ± 0.4 |
| + 300 g/L PEG 6k | 50.0 ± 2.6 | 6.9 ± 0.7 |
| + 300 g/L PEG 20k | 51.3 ± 0.6 | 7.8 ± 0.4 |
| HeLa cytosol ($n = 9$) | 50.5 ± 3.2 | 10.8 ± 4.5 |
| HeLa nucleus ($n = 13$) | 47.9 ± 3.8 | 7.3 ± 3.8 |

* In low ionic buffer (15 mM $\text{K}_x\text{H}_y\text{PO}_4$, pH 6.5, 25mM KCl) T_m of 4U and lm-4U were reported to be 41.1 °C and 35.9 °C, respectively.⁷

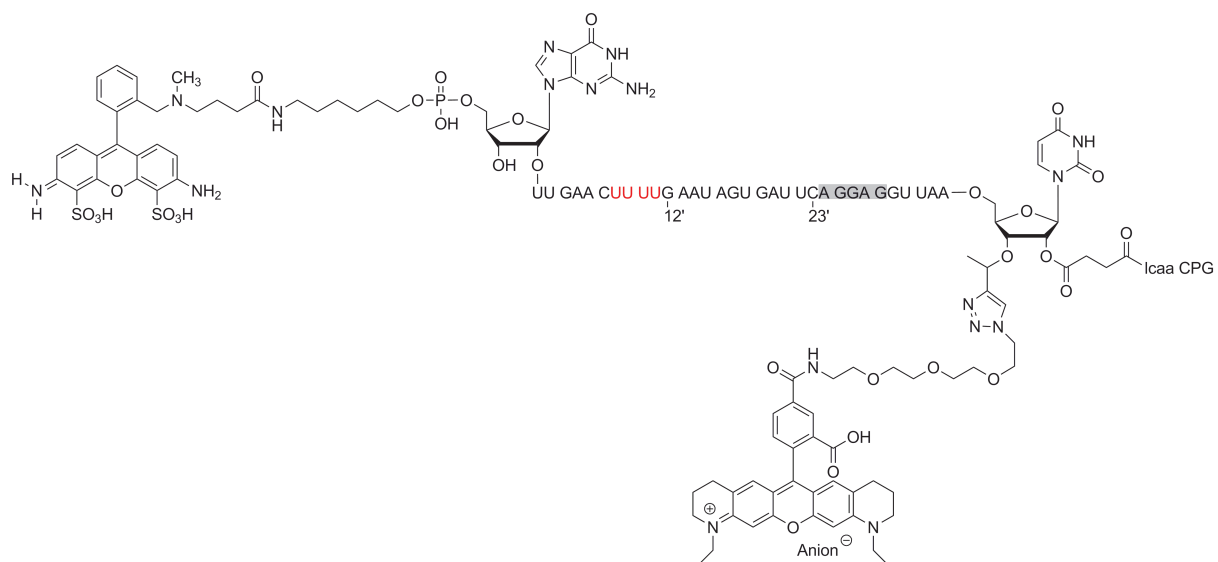


Figure S1. Structural formula of 4U RNA labeled with Atto488 and Atto565. The four consecutive U nucleotides are shown in red, the Shine-Dalgarno sequence in grey.

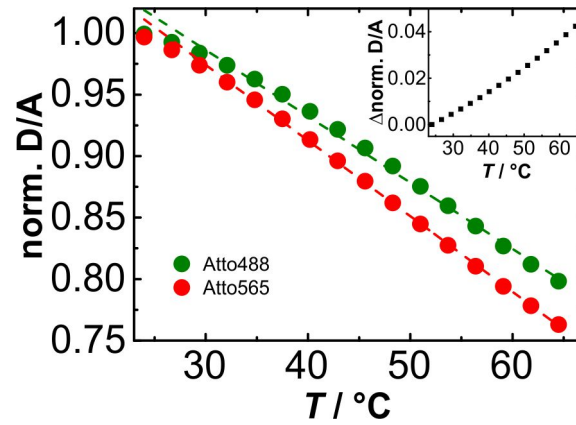


Figure S2. Intrinsic temperature dependence of Atto488 and Atto565. Normalized fluorescence intensities of Atto488 and Atto565 as function of temperature showed a linear trend. The slopes for Atto488 and Atto565 were $(-0.005 \pm 0.0001)/^{\circ}\text{C}$ and $(-0.006 \pm 0.00004)/^{\circ}\text{C}$, respectively and thus indicated a higher temperature dependency for Atto565 than Atto488. *Inset:* Calculated intrinsic response of the D/A with increasing temperature.

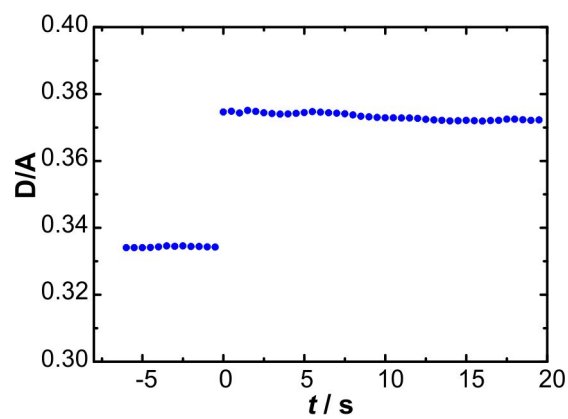


Figure S3. Representative time-resolved response of the D/A FRET-signal to a 2.4 °C temperature jump near to the melting temperature (at $t = 0$ s). The folding kinetics were completely equilibrated within the measured timescale.

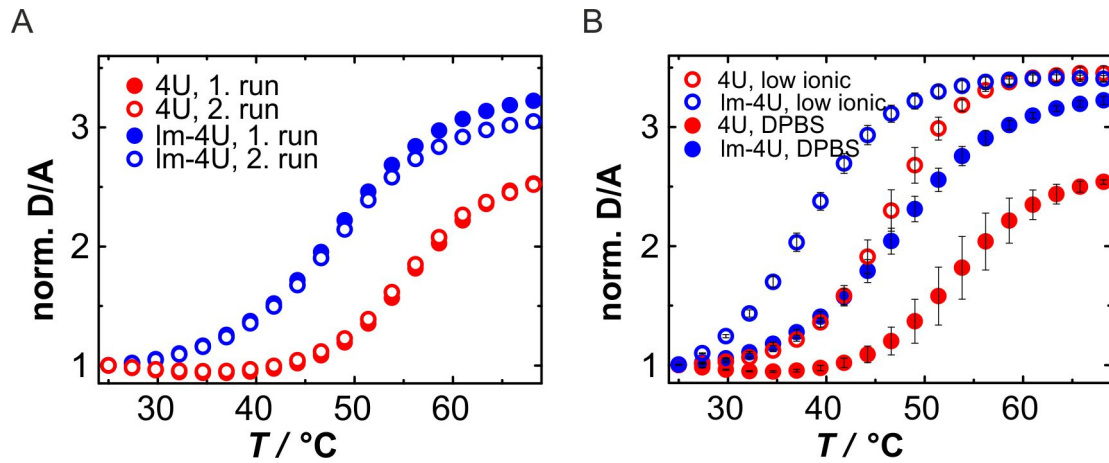


Figure S4. Thermal melting curves of the 4U RNA (4U) and its low-melting variant G12A-C23U variant (Im-4U) *in vitro*. (A) Reversibility of the unfolding transition shown by two consecutive temperature scans. (B) Melting curves of the 4U and Im-4U under different buffer conditions. The melting temperature of both hairpins was elevated in DPBS, pH 7.4 (8.1 mM Na_2HPO_4 , 1.5 mM KH_2PO_4 , 2.7 mM KCl, 136.9 mM NaCl) compared to that in a low ionic buffer, pH 7.4 (15 mM $\text{K}_x\text{H}_y\text{PO}_4$, 25 mM KCl). $n = 3-4$. Error bars represent mean \pm s.d.

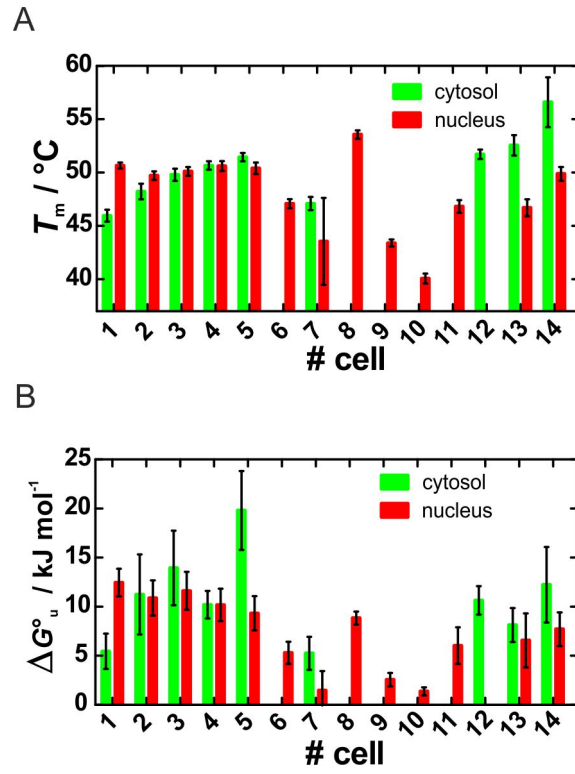


Figure S5. (A) Melting temperature (T_m) and (B) free energy change of unfolding at 37 °C (ΔG_u°) of Im-4U RNA averaged for different single cells over the nucleic and cytosolic regions. Error bars represent the fitting errors for the respective variables.

References

- (1) N. Rublack, H. Nguyen, B. Appel, D. Springstube, D. Strohbach, S. Müller, S. J. *Nucleic Acids* **2011**, *2011*, 805253.
- (2) W. Zhang, M. W. Capp, J. P. Bond, C. F. Anderson, M. T. Record, *Biochemistry* **1996**, *35*, 10506–10516.
- (3) M. Guo, Y. Xu, M. Gruebele, *Proc. Natl. Acad. Sci. USA* **2012**, *109*, 17863–17867.
- (4) S. Ebbinghaus, A. Dhar, J. D. McDonald, M. Gruebele, *Nat. Methods* **2010**, *7*, 319–323.
- (5) T. Vöpel, R. Scholz, L. Davico, M. Groß, S. Büning, S. Kareth, E. Weidner, S. Ebbinghaus, *Chem. Commun.* **2015**, *51*, 6913–6916.
- (6) S. Nakano, H. Karimata, T. Ohmichi, J. Kawakami, N. Sugimoto, *J. Am. Chem. Soc.* **2004**, *126*, 14330–14331.
- (7) J. Rinnenthal, B. Klinkert, F. Narberhaus, H. Schwalbe, *Nucleic Acids Res.* **2011**, *39*, 8258-8270.